Cemef

October, 11th 2018, GDR TherMatHT, Lyon

Two-phase modeling using the phase field theory

Franck Pigeonneau and **Pierre Saramito** (LJK, Grenoble)

1. Scientific issues in two-phase flows

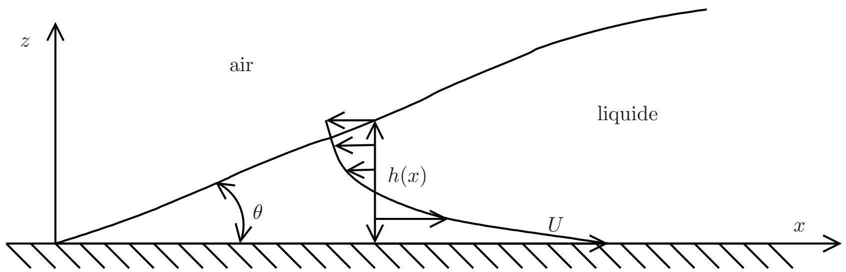

Figure 1: Fluid dynamics close to a contact line.

- The velocity gradient is:

$$\frac{\partial u}{\partial z} \approx \frac{U}{h(x)} = \frac{U}{\theta x} \tag{1}$$

- The viscous dissipation is given by[1]:

$$\Phi_\eta = \eta \int_\epsilon^R \left(\frac{\partial u}{\partial z}\right)^2 h dx = \eta \int_\epsilon^R \left(\frac{U}{h}\right)^2 h dx = \eta \frac{U^2}{\theta} \ln\left(\frac{R}{\epsilon}\right). \tag{2}$$

[1] P. G. De Gennes: Wetting: Statics and dynamics, in: Rev. Mod. Phys. 57.3 (1985), pp. 827–863.

1. Scientific issues in two-phase flows

- To remove the singularity:

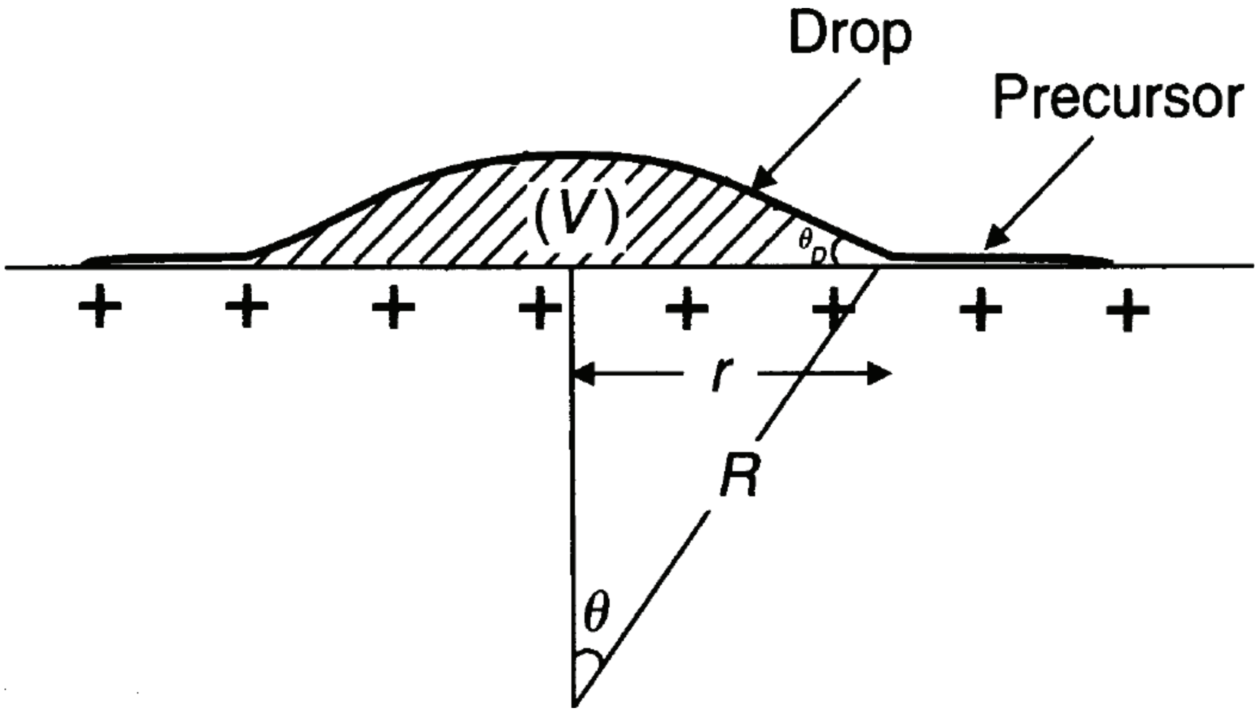

Figure 2: Precursor film[2].

[2] P.-G. De Gennes/F. Brochard-Wyart/D. Quéré: Gouttes, bulles, perles et ondes, Paris 2005.

1. Scientific issues in two-phase flows

- To remove the singularity:

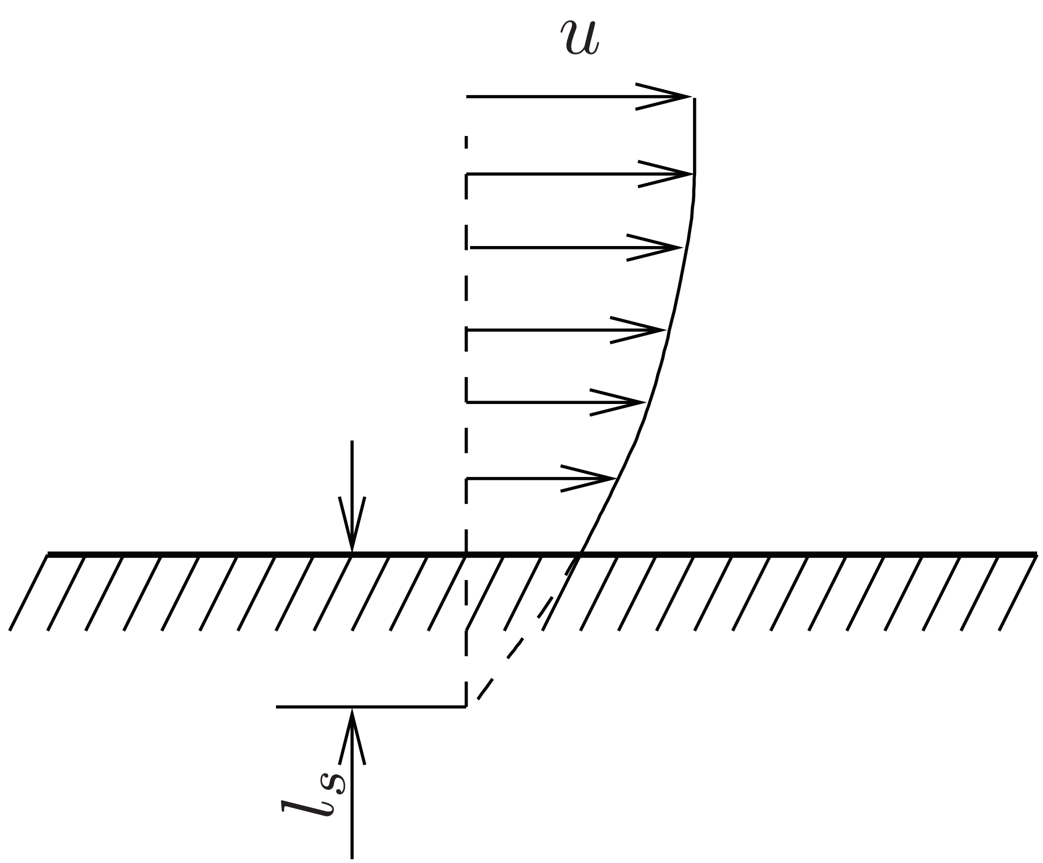

Figure 3: Slippage of fluids on wall[3].

[3] L. M. Hocking: A moving fluid interface. Part 2. The removal of the force singularity by a slip flow, in: J. Fluid Mech. 79.02 (1977), pp. 209–229.

1. Scientific issues in two-phase flows

- To remove the singularity:

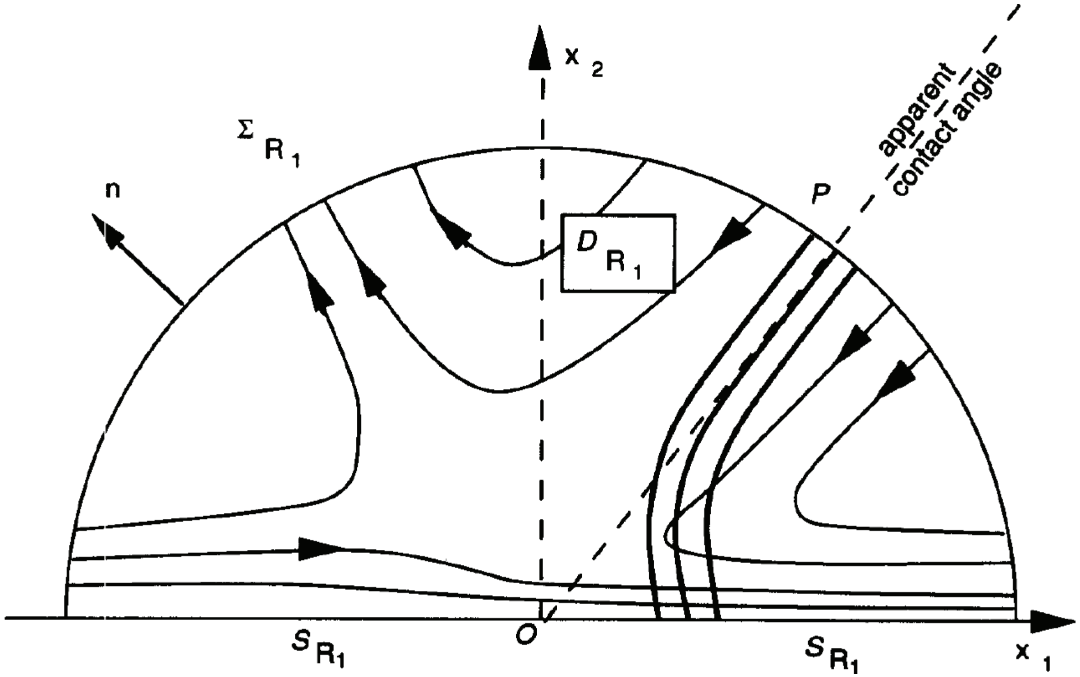

Figure 4: Contact line of diffuse interface[4].

[4] P. Seppecher: Moving contact lines in the Cahn-Hilliard theory, in: Int. J. Engng Sci. 34.9 (1996), pp. 977–992.

2. Basics of the phase field theory I

- Each phase is marked by a **"phase field"** or **"order parameter"**: φ.
- $\varphi = 1$ in phase 1 (ρ_1, η_1) and $\varphi = -1$ in phase 2 (ρ_2, η_2).

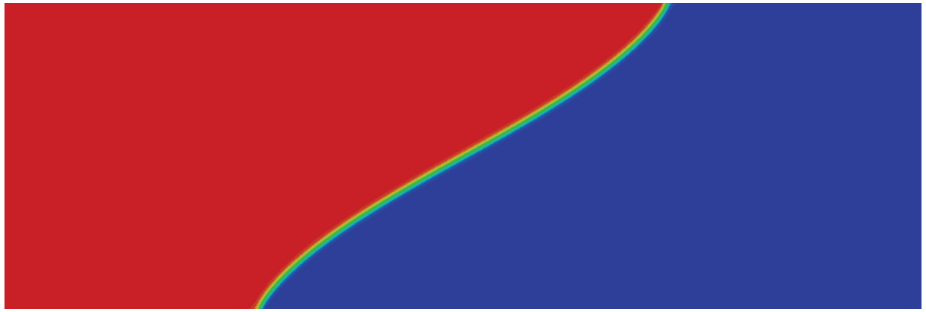

Figure 5: Shear flow with two phases.

$$\rho = \frac{\rho_1 + \rho_2}{2} + \frac{\rho_1 - \rho_2}{2}\varphi. \tag{3}$$

- The free energy is written as follows[5]

$$F[\varphi] = \int_\Omega \left[\Psi(\varphi) + \frac{k}{2} ||\nabla \varphi||^2 \right] dV. \qquad (4)$$

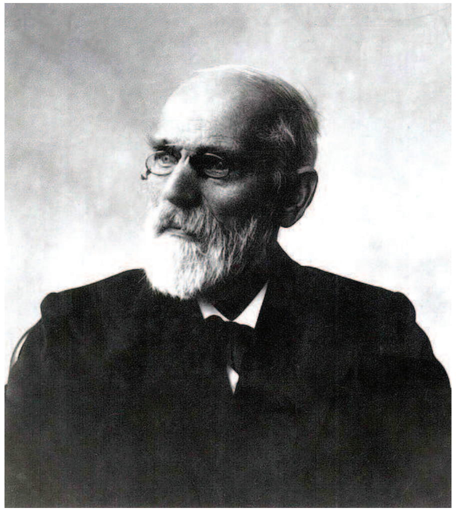

J. D. van der Waals (1837-1923).

- $\Psi(\varphi)$ is a double-well potential.

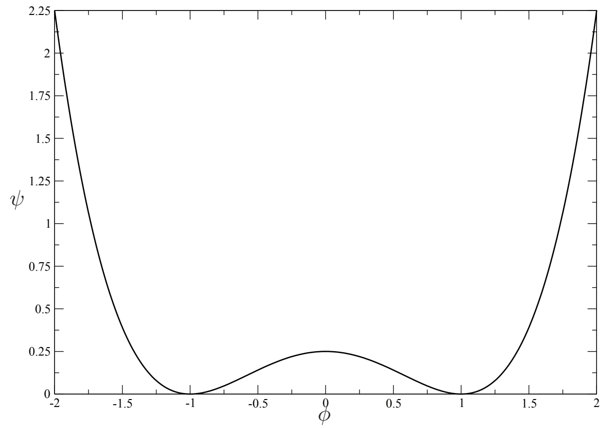

Figure 6: Example of a double-well potential: $\Psi = k(1-\varphi^2)^2/(4\zeta^2)$.

[5] J. D. van der Waals: The thermodynamic theory of capillarity under the hypothesis of a continuous variation of density, in: Verhandel. Konink. Akad. Weten. 1 (1893), pp. 1–56.

- At equilibrium, $F[\varphi]$ has to be minimal.

$$\delta F[\varphi] = \int_{\Omega} \left(\frac{d\Psi}{d\varphi} - k\nabla^2\varphi \right) \delta\varphi dV + \int_{\delta\Omega} \frac{\partial \varphi}{\partial n} \delta\varphi dS. \tag{5}$$

- Consequently:

$$\mu(\varphi) = \frac{d\Psi}{d\varphi} - k\nabla^2\varphi = 0, \ \forall \boldsymbol{x} \in \Omega, \tag{6}$$

$$k\frac{\partial \varphi}{\partial n} = 0, \ \text{sur } \delta\Omega. \tag{7}$$

- $\mu(\varphi)$ is the **chemical potential**.

2. Basics of the phase field theory

- In 1-dimension and with the previous double-well potential, the phase field is given by:

$$\varphi(\overline{x}) = \tanh\left(\frac{\overline{x}}{\sqrt{2}\,\mathrm{Cn}}\right), \tag{8}$$

$$\overline{x} = \frac{x}{L}, \tag{9}$$

$$\mathbf{Cn} = \frac{\zeta}{L}, \text{ Cahn number.} \tag{10}$$

- The surface tension is then defined by

$$\sigma = \frac{k}{L}\int_{-\infty}^{\infty}\left(\frac{d\varphi}{d\overline{x}}\right)^2 d\overline{x} = \frac{2\sqrt{2}k}{3\zeta}. \tag{11}$$

2. Basics of the phase field theory

- Outside the equilibrium, Cahn and Hilliard[6] proposed

$$\frac{\partial \varphi}{\partial t} = -\boldsymbol{\nabla} \cdot \boldsymbol{J}, \tag{12}$$

$$\boldsymbol{J} = -M\boldsymbol{\nabla}\mu, \tag{13}$$

$$\mu(\varphi) = \frac{d\Psi}{d\varphi} - k\boldsymbol{\nabla}^2\varphi. \tag{14}$$

- Time behavior of the phase field due to the diffusion of the chemical potential.
- Investigating spinodal decomposition.

[6] J. W. Cahn/J. E. Hilliard: Free Energy of a Nonuniform System. I. Interfacial Free Energy, in: J. Chem. Phys. 28.2 (1958), pp. 258–267.

2. Basics of the phase field theory

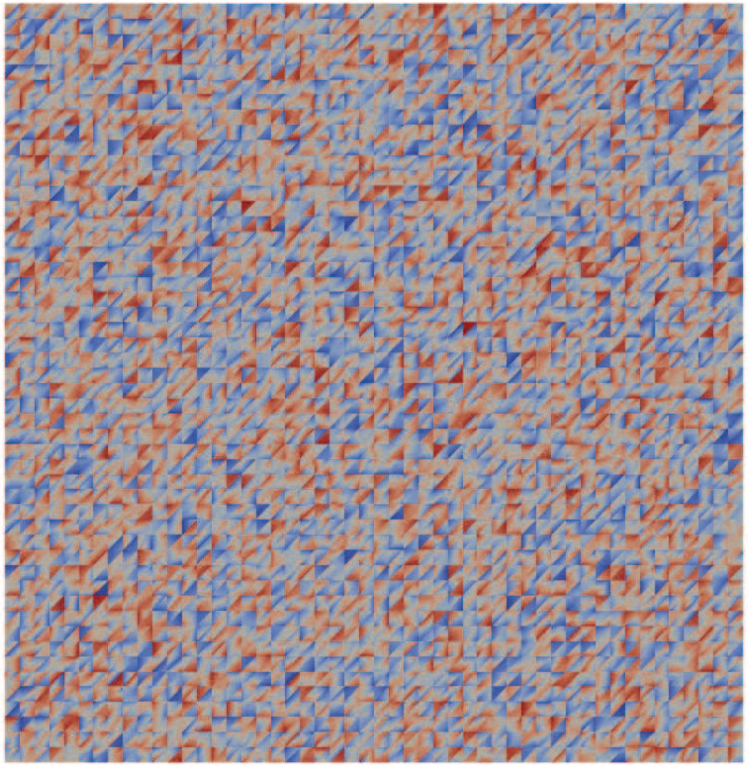

Numerical simulation of a spinodal decomposition in 2D, $\mathrm{Cn} = 10^{-2}$.

2. Basics of the phase field theory I

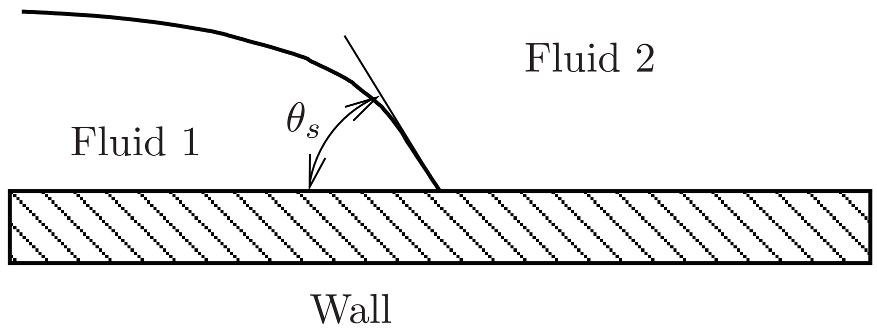

Figure 7: Contact line between two fluids and a wall. The static contact angle is θ_s.

$$F[\varphi] = \int_{\Omega} \left[\Psi(\varphi) + \frac{k}{2} ||\nabla \varphi||^2 \right] dV + \int_{\partial \Omega_w} f_w(\varphi) dS. \tag{15}$$

2. Basics of the phase field theory II

- The minimization of $F[\varphi]$[7]

$$\mu(\varphi) = \frac{d\Psi}{d\varphi} - k\boldsymbol{\nabla}^2\varphi = 0, \ \forall \boldsymbol{x} \in \Omega, \tag{16}$$

$$L(\varphi) = k\frac{\partial\varphi}{\partial n} + \frac{df_w}{d\varphi} = 0, \ \text{on } \partial\Omega_w. \tag{17}$$

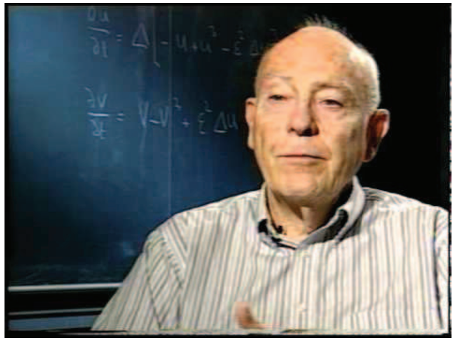

J. W. Cahn (1928-2016).

$$f_w(\varphi) = -\sigma\cos\theta_s\frac{\varphi(3-\varphi^2)}{4}, \tag{18}$$

$$k\frac{\partial\varphi}{\partial n} = \frac{3(1-\varphi^2)\sigma}{4}\cos\theta_s, \ \text{on } \partial\Omega_w. \tag{19}$$

[7] J. W. Cahn: Critical point wetting, in: J. Chem. Phys. 66.8 (1977), pp. 3667–3672.

2. Basics of the phase field theory

- Outside the equilibrium, creation of force proportional to $\mu\nabla\varphi$.
- Stokes equations:

$$\nabla\cdot\boldsymbol{u}=0, \tag{20}$$

$$-\nabla P+\nabla\cdot[2\eta(\varphi)\boldsymbol{D}(\boldsymbol{u})]+\rho(\varphi)\boldsymbol{g}+\mu\nabla\varphi=0, \tag{21}$$

- Cahn-Hilliard equation:

$$\frac{\partial\varphi}{\partial t}+\nabla\varphi\cdot\boldsymbol{u}=\nabla\cdot[M(\varphi)\nabla\mu(\varphi)], \tag{22}$$

$$\mu(\varphi)=\frac{\lambda}{\zeta^2}\left[\varphi(\varphi^2-1)-\zeta^2\nabla^2\varphi\right]. \tag{23}$$

2. Basics of the phase field theory

- Under dimensionless form:

$$\nabla \cdot \boldsymbol{u} = 0, \quad (24)$$

$$-\nabla P + \nabla \cdot [2\eta(\varphi)\boldsymbol{D}(\boldsymbol{u})] + \frac{\mathrm{Bo}}{\mathrm{Ca}}\rho(\varphi)\boldsymbol{g} + \frac{3}{2\sqrt{2}\,\mathrm{Ca}\,\mathrm{Cn}}\mu\nabla\varphi = 0, \quad (25)$$

$$\frac{\partial\varphi}{\partial t} + \nabla\varphi \cdot \boldsymbol{u} = \frac{1}{\mathrm{Pe}}\nabla^2\mu(\varphi), \quad (26)$$

$$\mu(\varphi) = \varphi(\varphi^2 - 1) - \mathrm{Cn}^2\,\nabla^2\varphi, \quad (27)$$

- Dimensionless numbers:

$$\mathrm{Bo} = \frac{\rho_1 g L^2}{\sigma}, \quad (28) \qquad \mathrm{Ca} = \frac{\eta_1 U}{\sigma}, \quad (29) \qquad \mathbf{Pe} = \frac{U\zeta^2 L}{M\lambda}, \quad (30)$$

$$\mathrm{Cn} = \frac{\zeta}{L}, \quad (31) \qquad \hat{\rho} = \frac{\rho_2}{\rho_1}, \quad (32) \qquad \hat{\eta} = \frac{\eta_2}{\eta_1}. \quad (33)$$

3. Numerical results of two-phase flows

○ 3.1 Droplet shrinkage

- Study this effect of Cahn number on droplet shrinkage for fluids at rest.

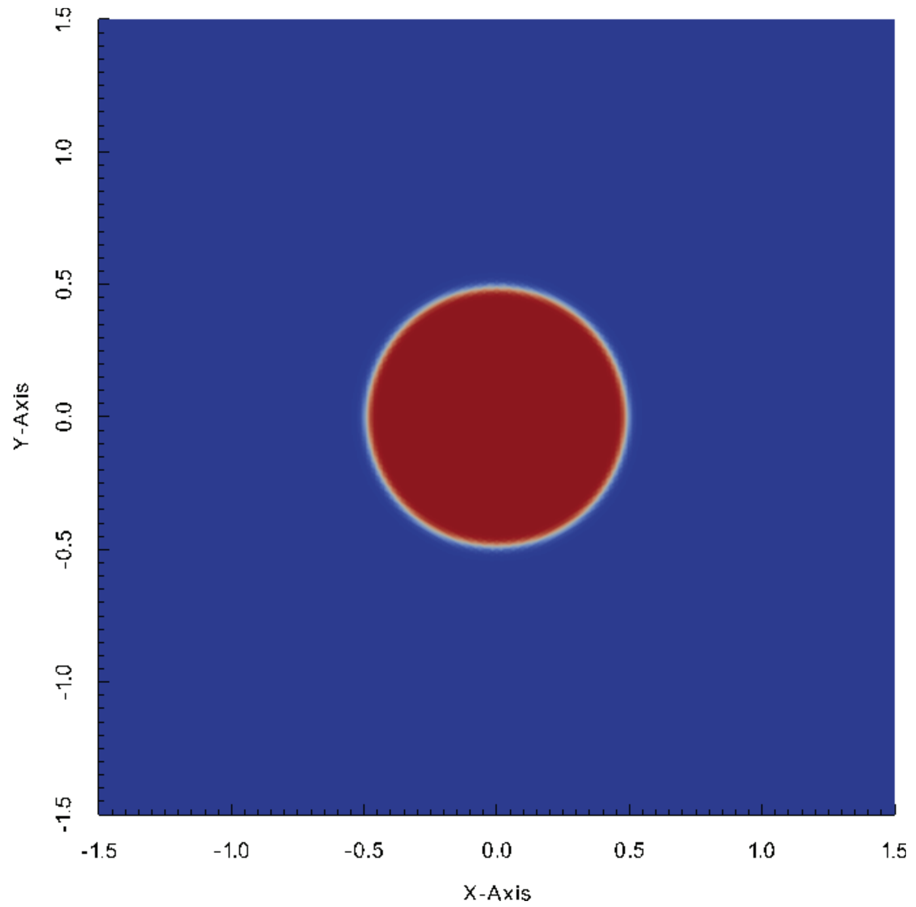

Figure 8: A static droplet in a liquid at rest.

3. Numerical results of two-phase flows

○ 3.1 Droplet shrinkage

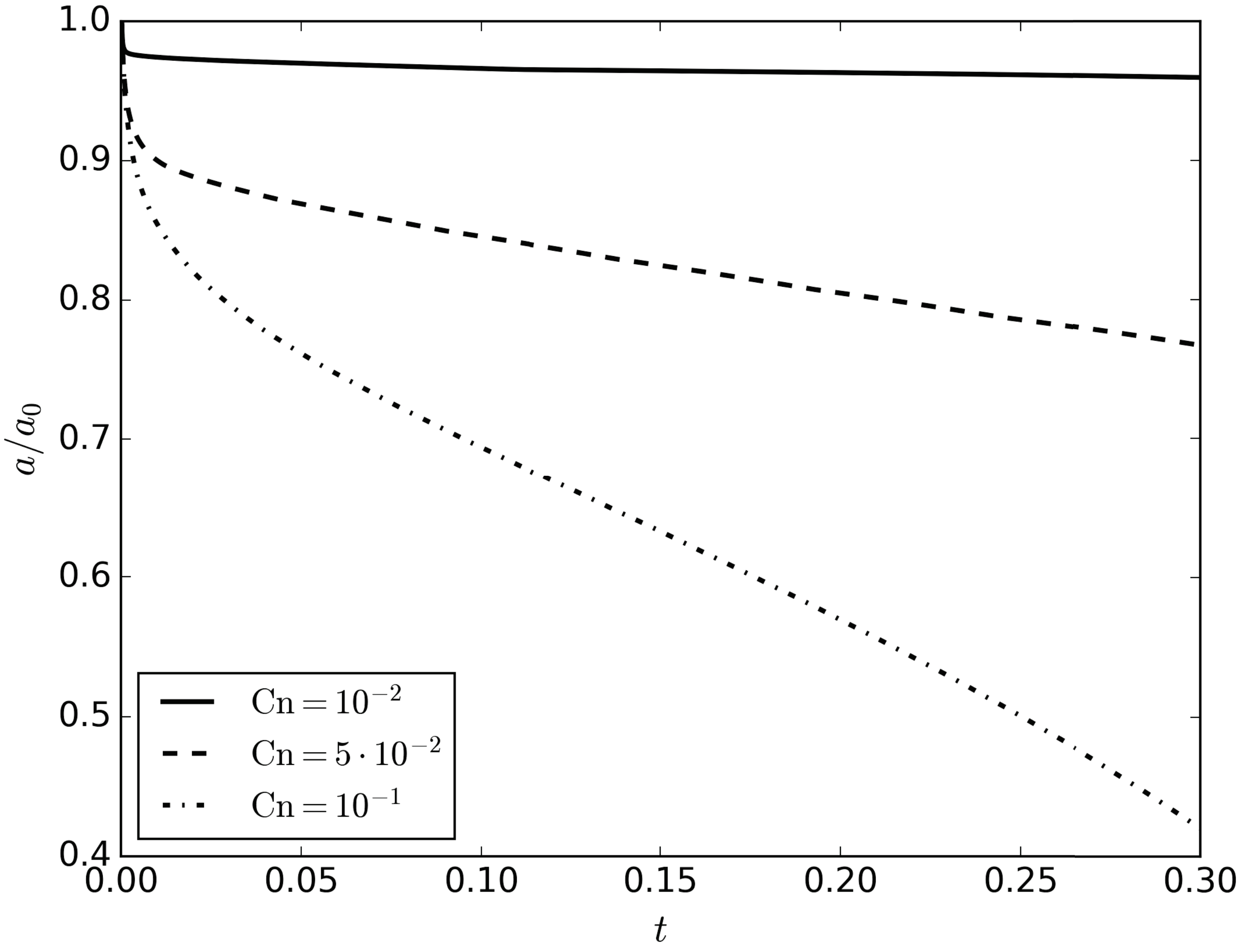

Figure 9: a/a_0 vs. t for three Cahn numbers.

3.1 Droplet shrinkage

- Small value of Cahn number prevents the shrinkage.
- According to Yue et al.[8], the critical radius below which the shrinkage occurs is

$$r_c = \sqrt[4]{\frac{2^{1/6}}{3\pi} V \, \mathrm{Cn}}, \quad (34)$$

  - $r_c = 0.7$ for $\mathrm{Cn} = 10^{-1}$,
  - $r_c = 0.6$ for $\mathrm{Cn} = 5 \cdot 10^{-2}$,
  - $r_c = 0.4$ for $\mathrm{Cn} = 10^{-2}$.

[8] P. Yue/C. Zhou/J. J. Feng: Spontaneous shrinkage of drops and mass conservation in phase-field simulations, in: J. Comput. Phys. 223.1 (2007), pp. 1–9.

○ 3.2 Capillary rising

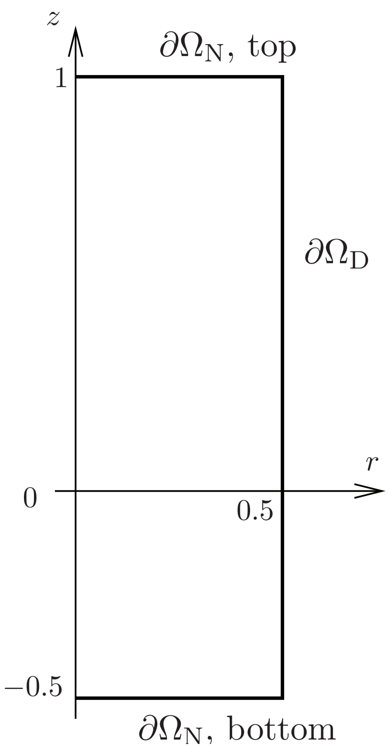

Figure 10: Geometry of the circular tube.

- The diameter of the tube is used as characteristic length.
- U chosen by balancing gravity $\sim$ viscous forces $\Rightarrow U = \rho g D^2/\sigma$.

$$\boldsymbol{u} = 0,\ \frac{\partial \varphi}{\partial n} = \frac{(1-\varphi^2)\sqrt{2}\cos\theta_s}{2\,\mathrm{Cn}},\ \frac{\partial \mu}{\partial n} = 0,\ \forall \boldsymbol{x} \in \partial\Omega_{\mathrm{D}}, \quad (35)$$

$$\boldsymbol{\sigma}\cdot\boldsymbol{n} = 0,\ \frac{\partial \varphi}{\partial n} = \frac{\partial \mu}{\partial n} = 0,\ \forall \boldsymbol{x} \in \partial\Omega_{\mathrm{N}},\ \text{top}, \quad (36)$$

$$\boldsymbol{\sigma}\cdot\boldsymbol{n} = -(\hat{\rho} + \frac{1}{2})\boldsymbol{n},\ \frac{\partial \varphi}{\partial n} = \frac{\partial \mu}{\partial n} = 0,\ \forall \boldsymbol{x} \in \partial\Omega_{\mathrm{N}},\ \text{bottom}. \quad (37)$$

3. Numerical results of two-phase flows

3.2 Capillary rising

- A numerical example has been done with:

$$\theta_s = 80^\circ,\ \mathrm{Bo} = 1,\ \mathrm{Cn} = 10^{-2},\ \mathrm{Pe} = 10^2. \tag{38}$$

- Initially, the heavy fluid (1) is below $z = 0$:

$$\varphi_0(z, r) = -\tanh\left(\frac{z}{\sqrt{2}\,\mathrm{Cn}}\right). \tag{39}$$

○ 3.2 Capillary rising

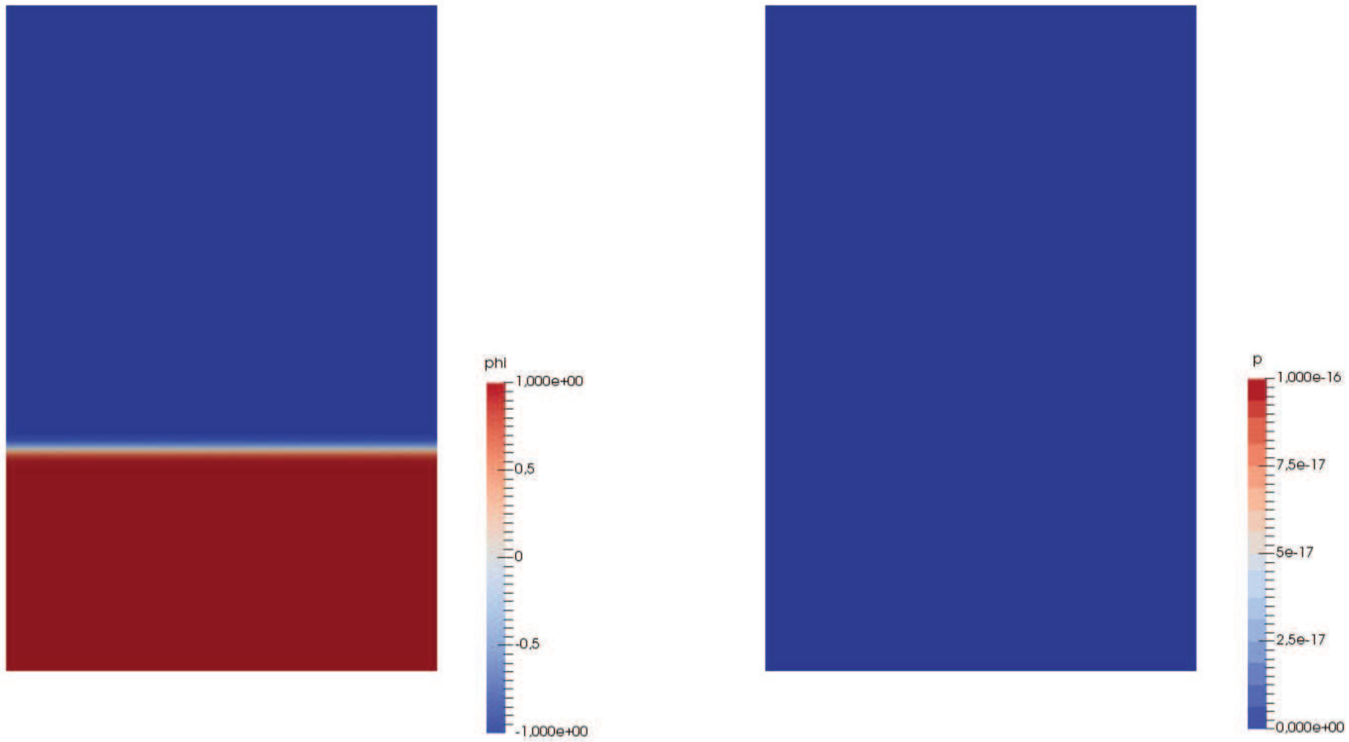

Capillary rising of water in a tube with a static contact angle equal to $4\pi/9$.

3. Numerical results of two-phase flows

○ 3.2 Capillary rising

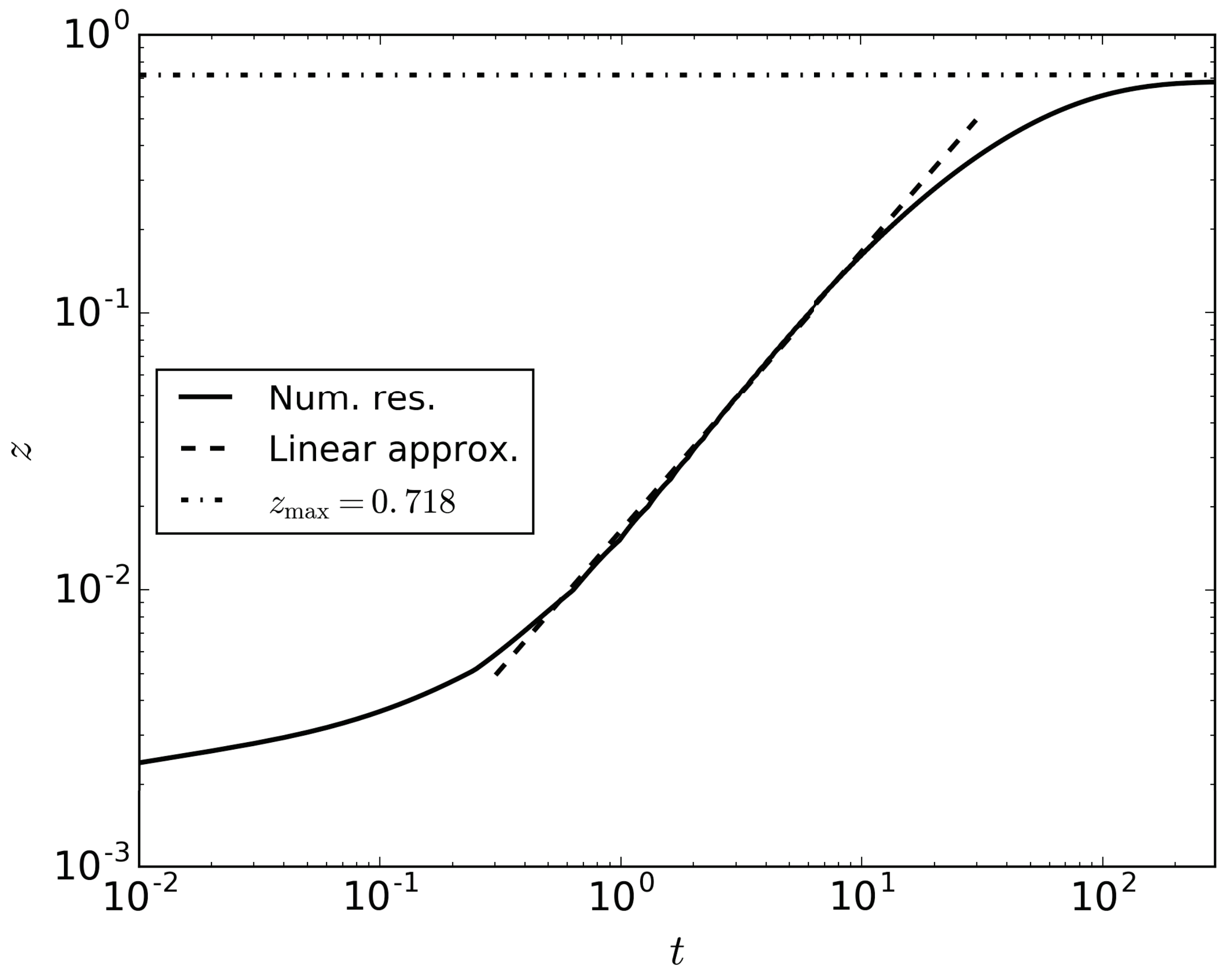

Figure 11: Contact line position as a function of time for $\theta_s = 80^\circ$ and $\mathrm{Bo} = 1$.

3. Numerical results of two-phase flows

○ 3.2 Capillary rising

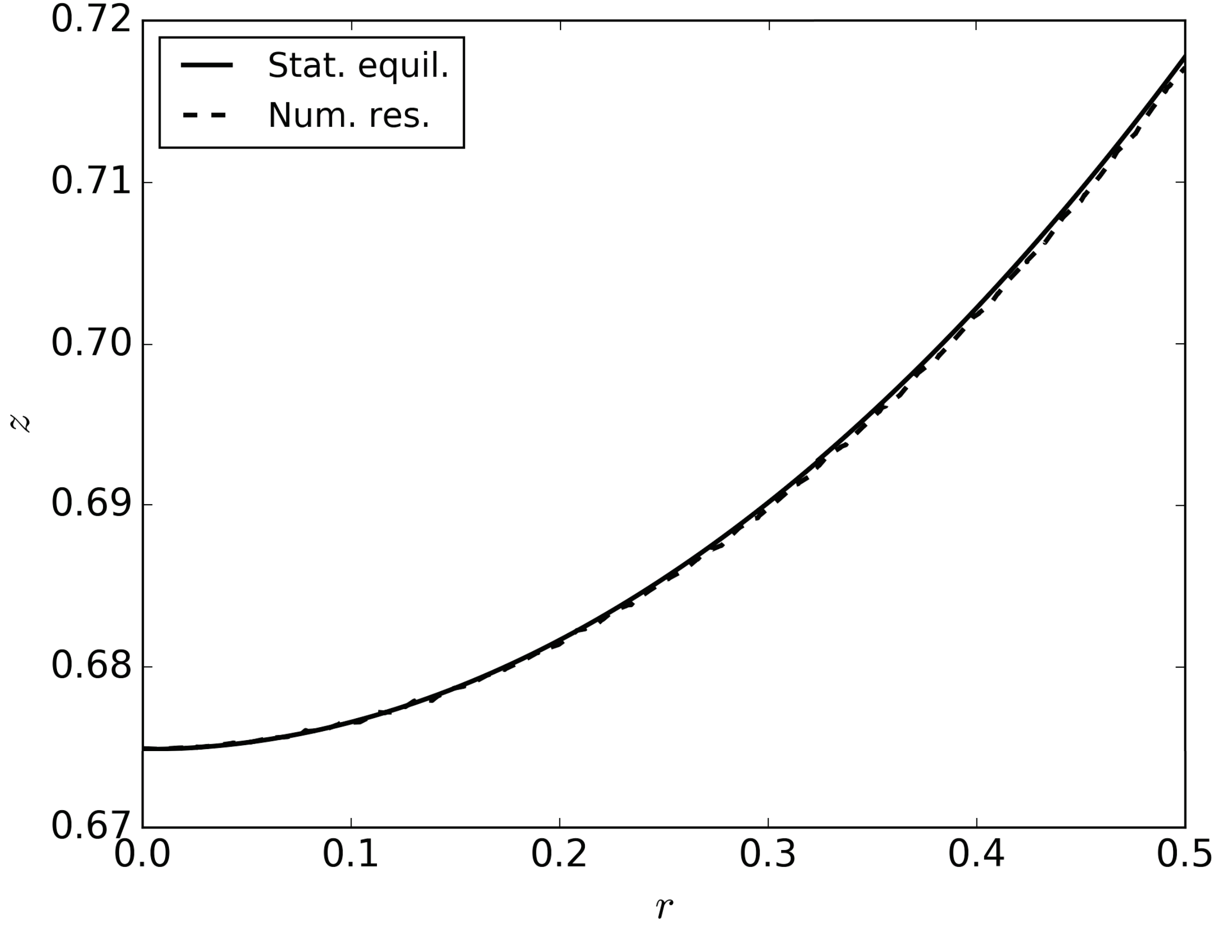

Figure 12: Geometry of the free surface, z vs. r, for $\theta_s = 80^\circ$ and $\mathrm{Bo} = 1$.

3. Numerical results of two-phase flows

○ 3.2 Capillary rising

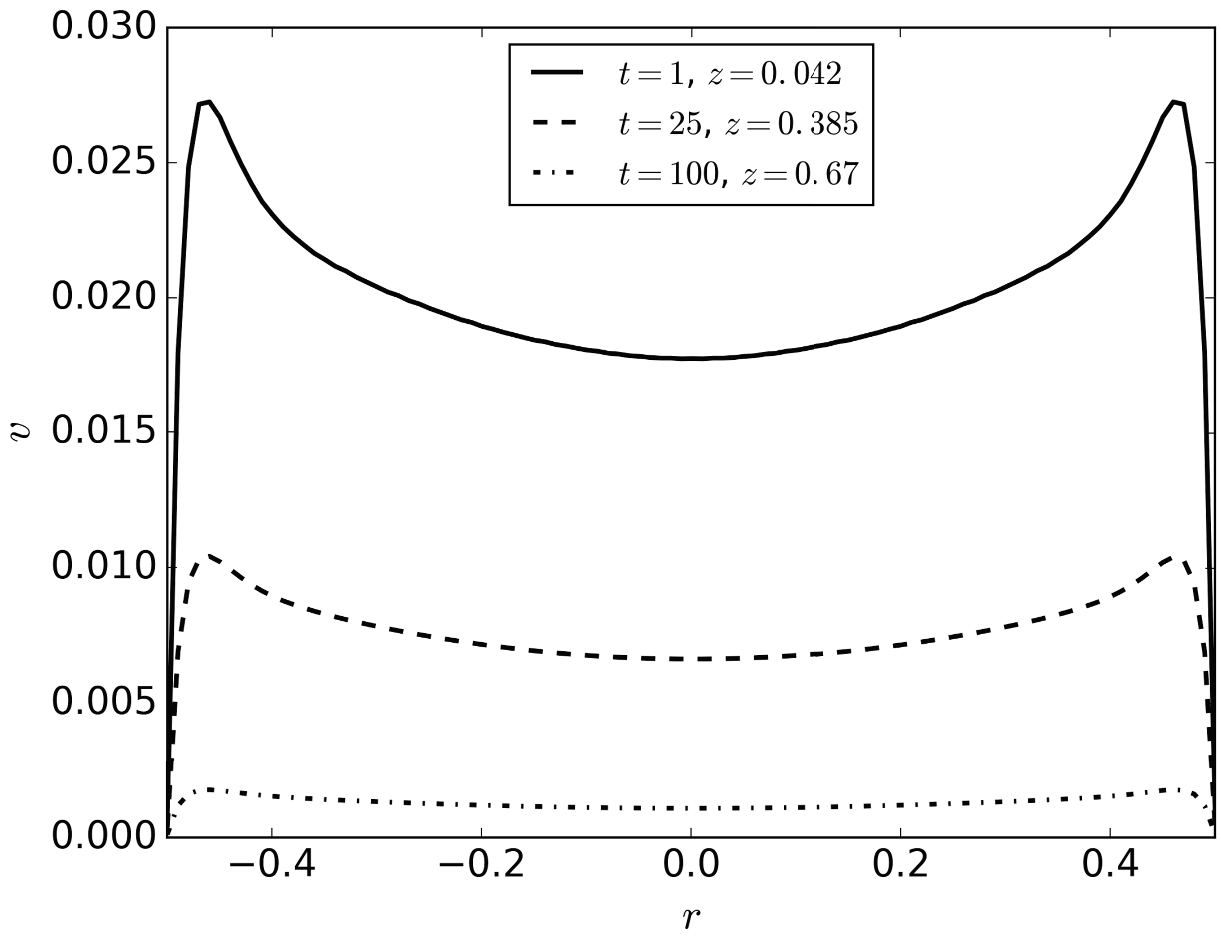

Figure 13: *z*-axis velocity component *v* vs. *r*, over an horizontal line localized right on the contact line.

○ 3.2 Capillary rising

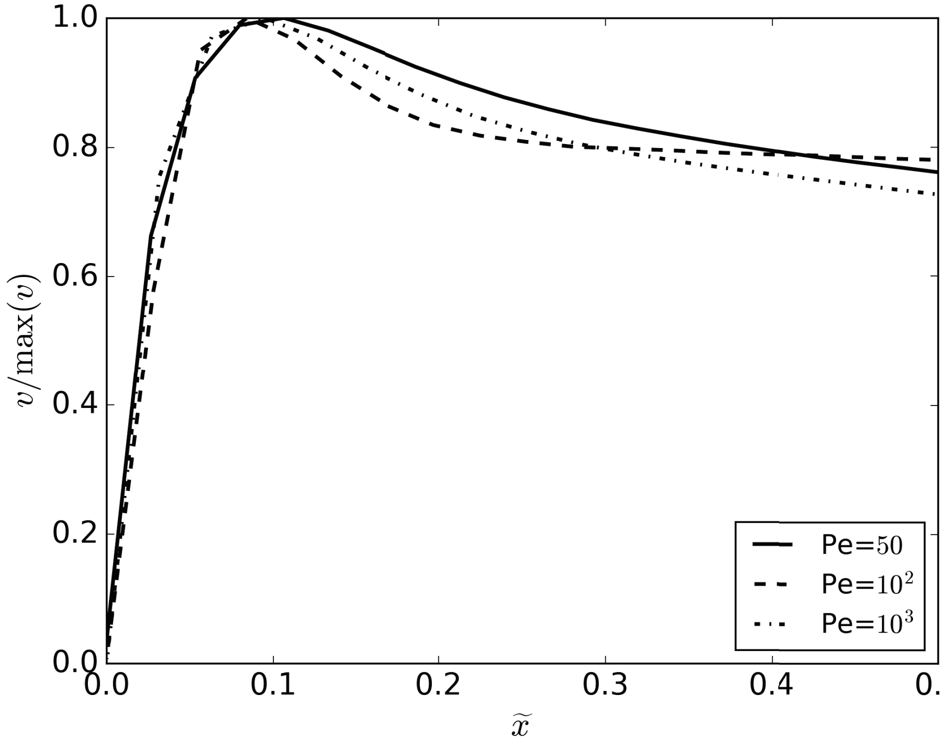

Figure 14: $v/\max(v)$ vs. $\widetilde{x} \sim \sqrt[4]{\mathrm{Pe}}$ right on the contact line for $t = 2.5$ for $\mathrm{Bo} = 1$ and $\mathrm{Pe} = 50$, 10^2 and 10^3.

- The diffusion layer of $\mu \sim 1/\sqrt[4]{\mathrm{Pe}}$ as shown in[9].

[9] A. J. Briant/J. M. Yeomans: Lattice Boltzmann simulations of contact line motion. II. Binary fluids, in: Phys. Rev. E 69 (3 2004), p. 031603.

○ 3.3 Drop spreading on an horizontal wall

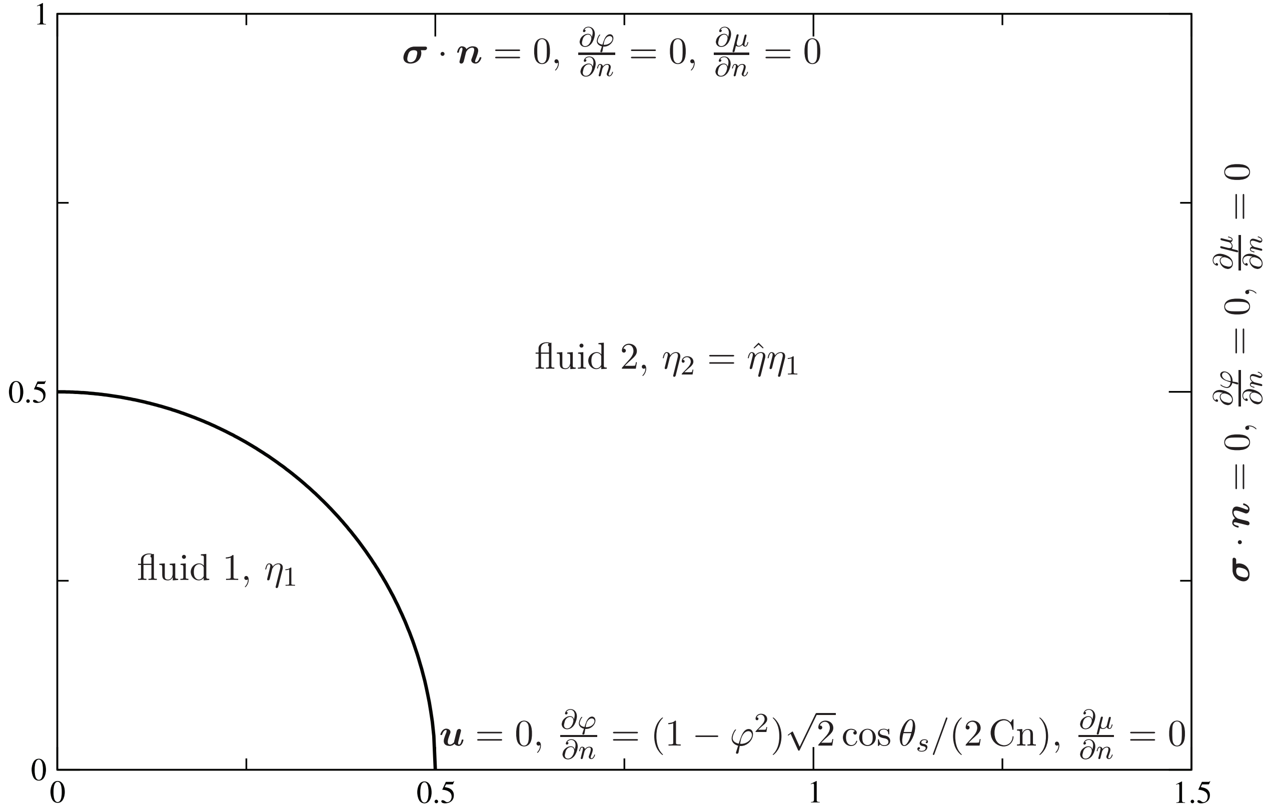

Figure 15: Geometry of a spreading drop of fluid 1 in the initial configuration.

3. Numerical results of two-phase flows

○ 3.3 Drop spreading on an horizontal wall

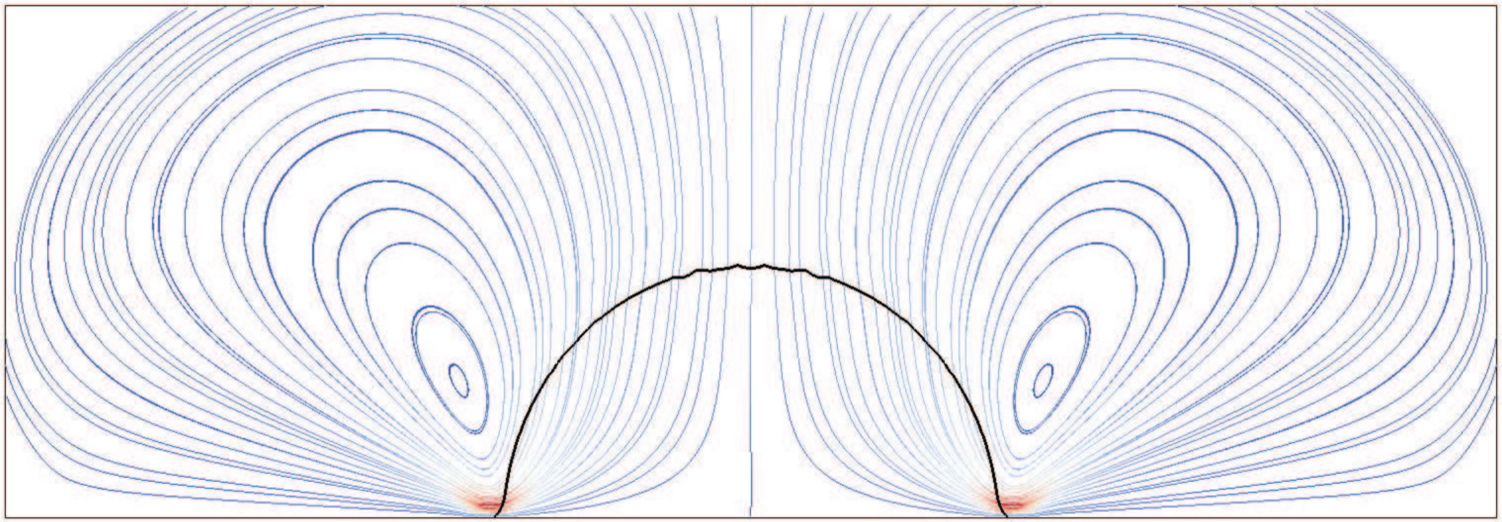

Drop spreading of a drop on a wall with $\theta_s = \pi/6$, $\mathrm{Cn} = 10^{-2}$ and $\mathrm{Pe} = 10^2$.

3. Numerical results of two-phase flows

○ 3.3 Drop spreading on an horizontal wall

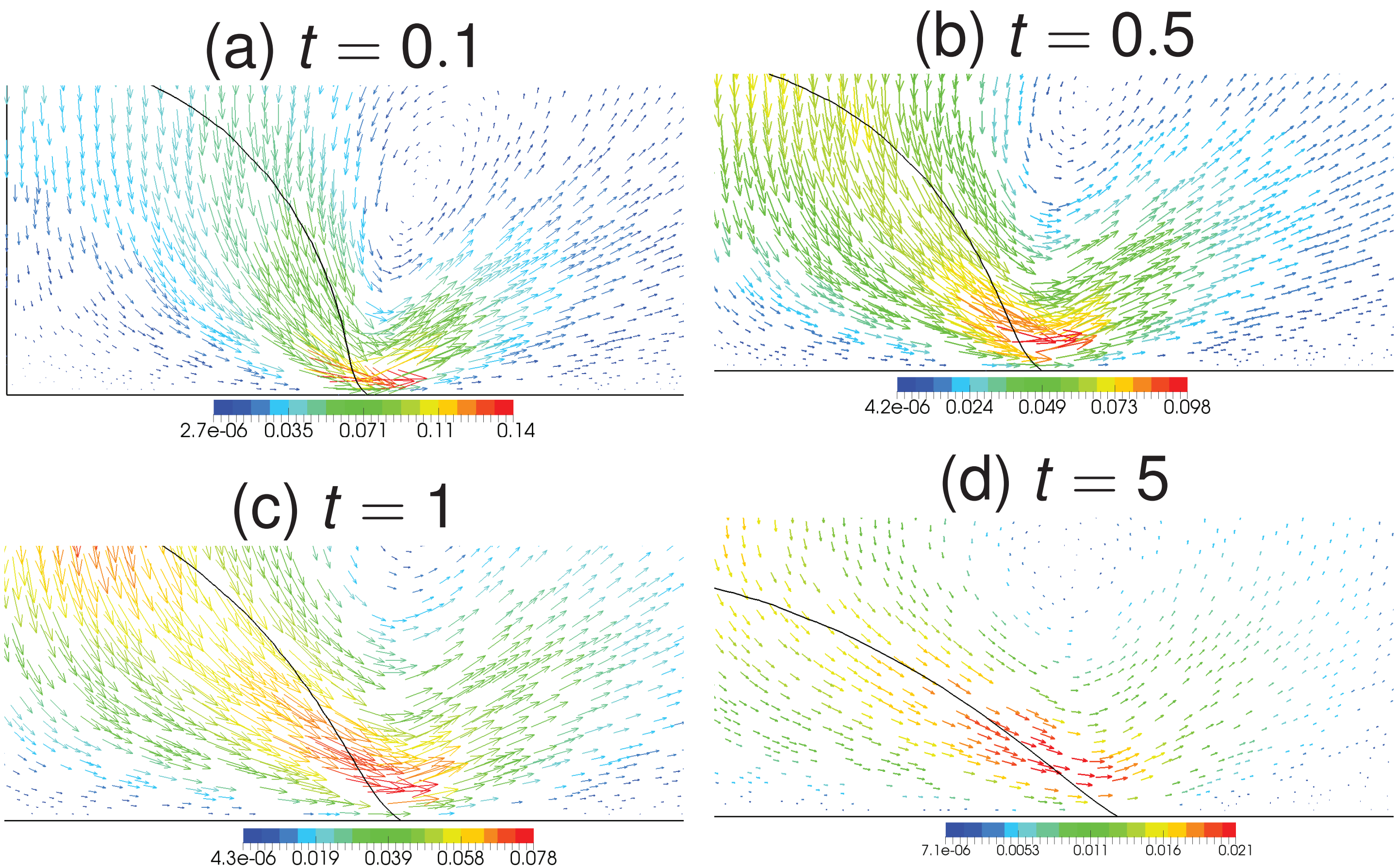

Figure 16: Velocity field in the neighbourhood of the triple line.

○ 3.3 Drop spreading on an horizontal wall

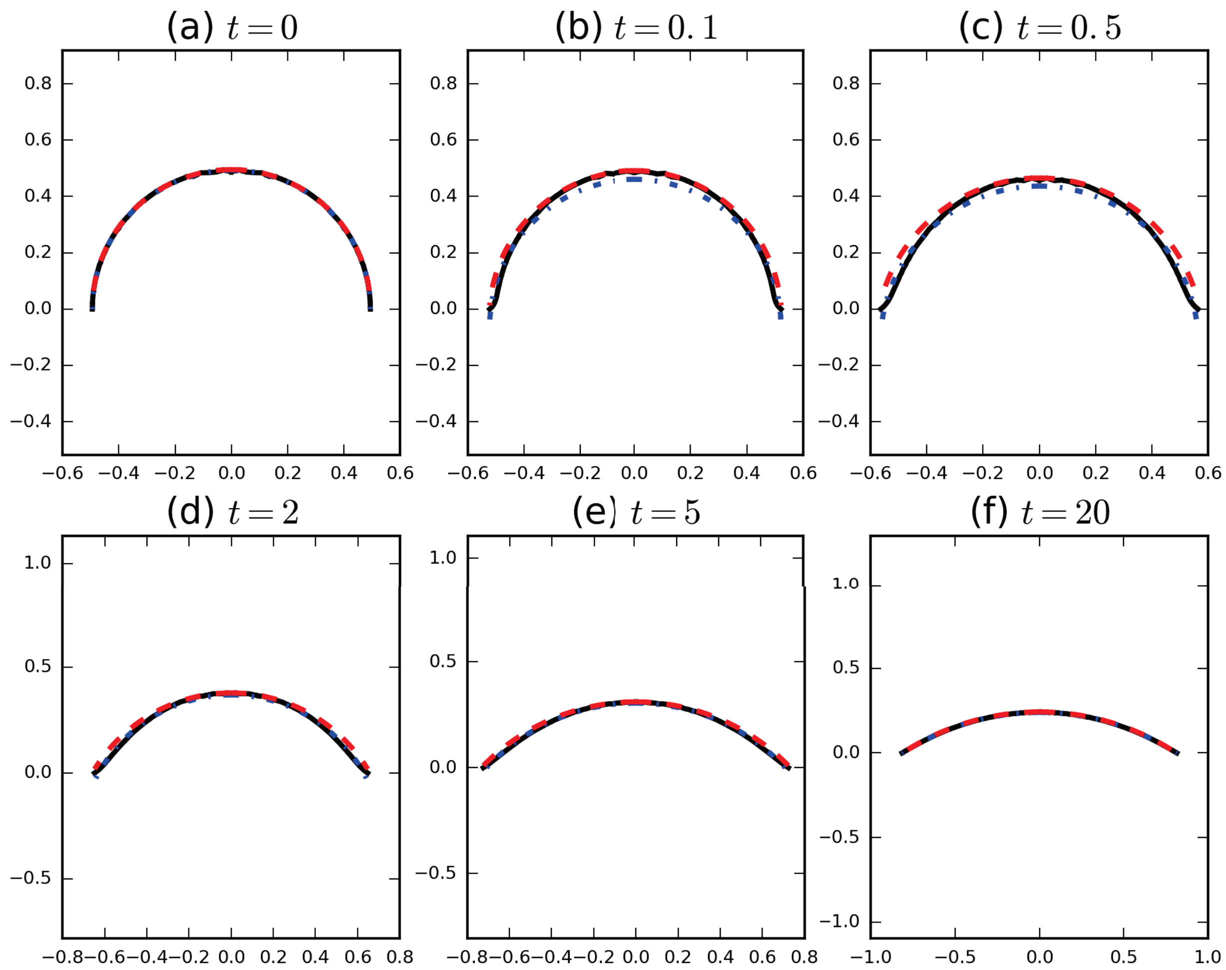

Figure 17: Drop shape during the spreading at different times.

○ 3.3 Drop spreading on an horizontal wall

- The theory of the dynamics of triple line has been described by Cox[10]:

$$g(\theta_d, \hat{\eta}) - g(\theta_s, \hat{\eta}) = -\mathrm{Ca}^* \ln \epsilon, \tag{40}$$

in which the function $g(\theta, \hat{\eta})$ is given by

$$g(\theta, \hat{\eta}) = \int_0^\theta \frac{d\alpha}{f(\alpha, \hat{\eta})}, \tag{41}$$

with

$$f(\alpha, \hat{\eta}) = \frac{2\sin\alpha \left\{ \hat{\eta}^2 \left(\alpha^2 - \sin^2\alpha \right) + 2\hat{\eta} \left[\alpha(\pi - \alpha) + \sin^2\alpha \right] + (\pi - \alpha)^2 - \sin^2\alpha \right\}}{\hat{\eta}(\alpha^2 - \sin^2\alpha)\left[\pi - \alpha + \sin\alpha\cos\alpha\right] + \left[(\pi - \alpha)^2 - \sin^2\alpha\right](\alpha - \sin\alpha\cos\alpha)}. \tag{42}$$

[10] R. G. Cox: The dynamics of the spreading of liquids on a solid surface. Part 1. Viscous flow, in: J. Fluid Mech. 168 (1986), pp. 169–194.

○ 3.3 Drop spreading on an horizontal wall

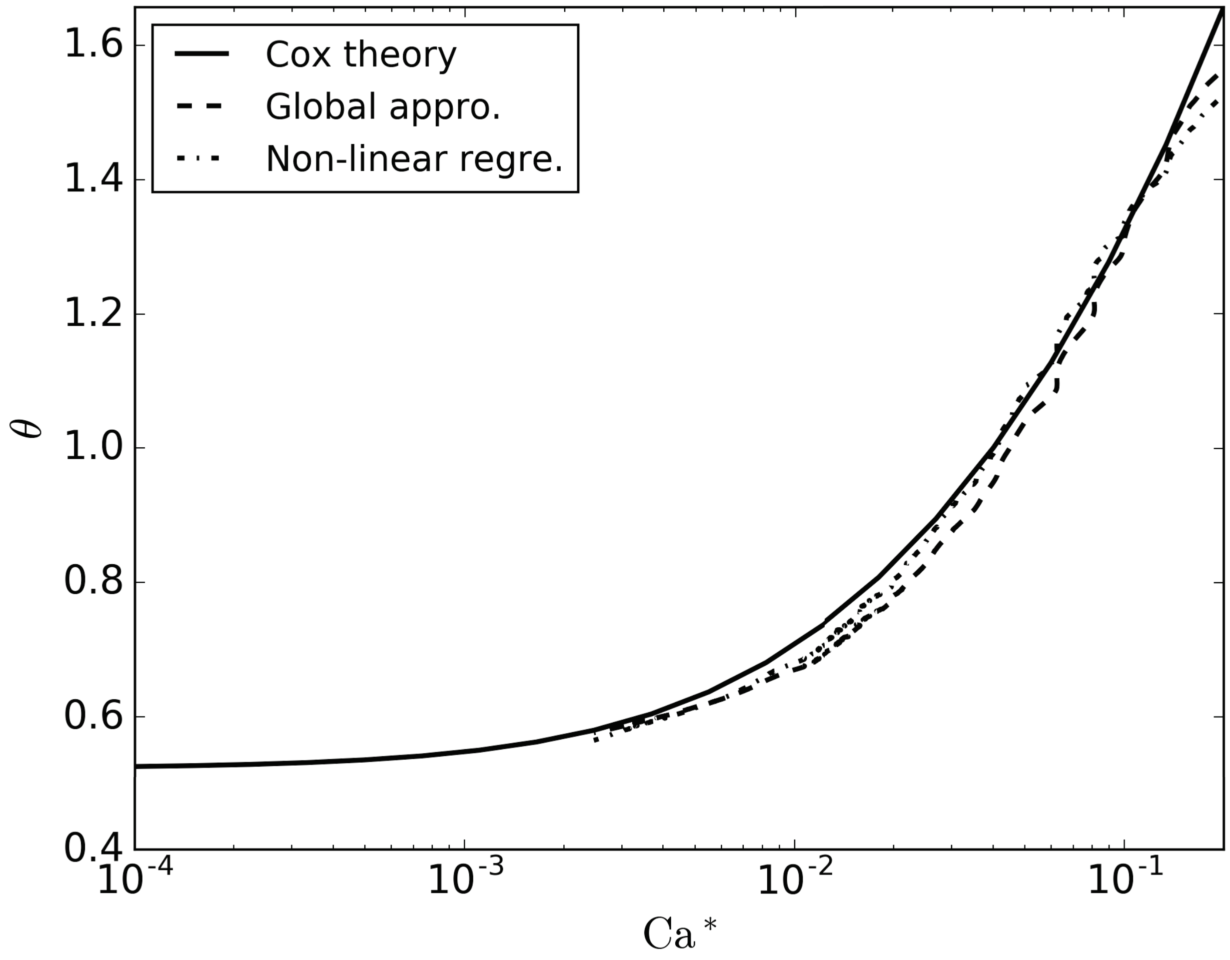

Figure 18: The dynamic contact angle as a function of Ca^*. Comparison between the numerical result and the Cox's theory with $\epsilon = 10^{-1}$.

4. Conclusion and perspectives

- Numerical solver to study two-phase flows using the phase field theory[11]:
  - Wetting properties of wall easy to take into account.
- Dynamics and temporal behaviors well described:
  - Capillary rising in a tube;
  - Drop spreading on a solid substrate.
- The physics is mainly controlled by two numbers:
  - $\mathrm{Cn} \leq 10^{-2}$; $\mathrm{Pe} \geq 10^{2}$.

- Introduce a “real” thermodynamics.
- Applications:
  - Phase separation of oxide glasses;
  - Bubble nucleation in glass former liquids.

[11] F. Pigeonneau/E. Hachem/P. Saramito: Discontinuous Galerkin finite element method applied to the coupled Stokes/Cahn-Hilliard equations, in: Int. J. Num. Meth. Fluids under revision (2018), pp. 1–28.